High Pressure Solvothermal Microencapsulation of D-Mannitol in Inorganic Shells for Thermal Energy Storage

ROXANA M. PITICESCU[1], LAURA M. POPESCU[1], ANCA E. SLOBOZEANU[1]*, ALBERT I. TUDOR[1], RADU R. PITICESCU[1], MARIA DOLORES ROMERO SANCHEZ[1]

[1] National R&D Institute for Nonferrous and Rare Metals, 102 Biruintei Blvd., Pantelimon, Ilfov, Romania

D-Mannitol has been demonstrated by different authors as a new phase change material (PCM) for thermal energy storage with high latent heat, low cost, environmentally friendly chemical nature and suitable melting temperature for applications in solar collectors, space heating or industrial waste heat. The main drawback is their low thermal conductivity, affecting heat transfer properties. In this work, the microencapsulation of D-Mannitol in ZnO shells is evaluated as a procedure to increase the specific area of heat exchange. The inorganic shell based on ZnO has been selected for the microencapsulation using an in-situ solvothermal followed by spray drying. Characterization of the microcapsules obtained has been mainly carried out by XRD, DSC, IR spectroscopy and SEM. Results have shown that experimental parameters such as the pressure and reaction time for the solvothermal microencapsulation process determine the crystalline phases of the shell and their thermal energy storage properties (melting temperature and enthalpy).

Keywords: Thermal Energy Storage, Sugar alcohol, Microencapsulation, D-Mannitol, Hydrothermal process.

Sugar alcohols, in particular D-Mannitol, are proposed by different authors as new materials for thermal energy storage applications, as they possess a convenient melting temperature for applications in solar collectors, space heating, industrial waste heat, etc. [1, 2]. Moreover, they are low-cost and environmentally friendly materials and with latent heat values comparable to those of paraffin waxes and hydrated salts [3-5].

However, in spite of their advantages as thermal energy storage materials, sugar alcohols, like most PCMs, impose an important drawback for the heat transfer due to their low thermal conductivity (generally <1 W/m K).

Premkumar et al. and Sari [6, 7] demonstrated the effectiveness of macroencapsulated D-Mannitol as thermal energy storage system (TES) using fatty acids compounds as organic solid-liquid PCMs; however melting temperatures of the PCMs were in the range of 42-65°C, far from the melting temperature of D-Mannitol (166°C).

Microencapsulation of PCMs, including D-Mannitol, is considered as an appropriate and promising option as microcapsules with high specific surface for heat exchange are obtained for thermal energy storage [2,3, 8-11].

There is a wide number of physical, chemical or physical-chemical processes developed for particles micro-encapsulation in different industrial sectors and applications (cosmetic, food, pharmaceutical, etc) [12-15]. The selection of the most suitable microencapsulation method depends on the core substance to be encapsulated and the shell material, as well as on the required morphology, particle size or surface characteristics [16, 17].

Interfacial polycondensation has been proposed by different authors for the encapsulation of different core materials [18], who have demonstrated the great amount of parameters affecting the properties of the microparticles synthetized. In particular this technique has been successfully used for the synthesis of sugar alcohols microparticles with a polyurea-urethane shell [19, 20], their molar ratio determining the shell thickness [21-23]. In the case of D-Mannitol as core material, the main problem is its high water solubility, which makes more difficult the encapsulation into a polyurethane shell by interfacial polycondensation.

Microencapsulation using inorganic shells for microencapsulation of different compounds using AlOOH, TiO_2, ZnO, Au, Ag and Cu has been reported [24-26]. In recent years, ZnO is growing attention due to its chemical and temperature stability, low dielectric constant, high catalysis activity, antibacterial and bactericide, semiconductor, piezoelectrics, etc) [27, 28]. Hydrothermal method [29] and co-precipitation [30] were used for obtaining Ag/ZnO, TiO_2/ZnO or chitosan/ZnO core/shell particles [31- 34].

The size and concentration of the D-Mannitol as core material strongly influences the physical, chemical and biological properties of core/shell particles [35-39]. Under the best of our knowledge any reference in literature has been found on the encapsulation of sugar alcohols using ZnO as inorganic shell. The feasibility of this type of encapsulation by solvothermal methods has been studied in this paper, considering the influence of pressure on the formation of ZnO-D-Mannitol composites (crystallisation, morphology).

Experimental part

Zinc nitrate hexahydrate, $Zn(NO_3)_2 \cdot 6H_2O$ (Merck) was used as precursor for the synthesis of ZnO shell by solvothermal process. D-Mannitol ($C_6H_{14}O_6$, >98%, MP=167-170°C, Merck) was used as PCM core material. Ethyl alcohol solution 98% and ammonium hydroxide solution 25% were used as synthesis reagents.

A process based on the *in-situ* solvothermal synthesis of ZnO in the presence of the sugar alcohol followed by spray drying has been propopsed. The selection of ZnO as inorganic shell material for the microencapsulation of D-Mannitol has been done taking into account: (i) ability to be obtained by in alcohol solutions avoiding dissolution of D-Mannitol during encapsulation; (ii) chemical compatibility with sugar alcohol enhancing the stability of

---

* email: a.slobozeanu@imnr.ro; Phone: +40213522048

the microcapsules and (iii) possibility to control shell morphology. The quantity of ZnO was calculated based on the following equation, considering both core particles and inorganic shell with spherical shape:

$$\delta_{shell} = \frac{6M_{ZnO}\rho_{S.A}}{M_{S.A}\rho_{ZnO}} d_{core} \qquad (1)$$

where: δ_{shell} is the targeted shell thickness, M_{ZnO} is the molecular weight of shell; $M_{S.A}$ is the molecular weight of sugar alcohol encapsulated; ρ_{ZnO} is the density of the shell (particularly ZnO in this case); $\rho_{S.A}$ is the density of the encapsulated sugar alcohol; d_{core} is the diameter of the encapsulated sugar alcohol particles.

Solvothermal precipitation of the shell is based on the nucleation of ZnO from the $Zn(OH)_4^{2-}$ nuclei formed according to the reaction [29].

$$Zn(OH)_4^{2-} = ZnO + H_2O + 2OH^- \qquad (2)$$

Further on, precipitated white slurry of ZnO inorganic precursor was mixed in ethanol medium with spray dried D-Mannitol and solvothermally treated at 100°C for 1-3 h at pressures in the range 40-100 atm. (Berghof autoclave, Germany, model BR-4000, with temperature controller and data acquisition) and high pressure range of 1000-3000 atm. (HP System autoclave France, PID controller). Weight ratio between ZnO and D-Mannitol was varied with the aim to optimize synthesis conditions by avoiding the formation of secondary phases.

Spray drying processing of the wet precipitates removed from the autoclave was done on a LabPlant system with 0.5 mm nozzle size in hot air, leading to the formation of relatively rounded morphologies for the ZnO-D-Mannitol systems.

Evaluation of the crystalline structure has been carried out by X-Ray Diffraction (XRD, Bruker-AXS D8 Advance Diffractometer) with monochromatic CuKα radiation. Scans were obtained in the range $2\theta = 4 \div 74°$, with a step size of 0.02° every 2 s.

The FT-IR spectra of the microcapsules obtained with the ZnO shell was recorded using an ABB MB3000 spectrometer in transmission mode between 4000 and 550 cm^{-1} (64 scans with 4 cm^{-1} resolution).

The surface morphology was obtained using an optical microscope Axio Imager A1M Carl Zeiss in polarised light and Tecnai G2 F30 for the S-TEM microscopy.

Thermal properties of the microcapsules obtained were measured by using the SETARAM Setsys Evolution equipment for the DSC-TG experiments with heating rate of 10°C/min under argon atmosphere from 20 to 600°C.

Results and discussions

In a first step, the feasibility of microencapsulation of D-Mannitol within ZnO inorganic shell obtained by solvothermal methodology has been studied by analysing the properties of the microparticles with different ZnO: D-Mannitol ratios. Table 1 includes sample nomenclature and ZnO: D-Mannitol ratio as well as the melting temperature (T_m) and enthalpy (ΔH_m) obtained by DSC for the samples synthetized at the following parameters: pressure P=100 atm, temperature T=120°C, duration t= 2 h.

For the highest ratio ZnO: D-Mannitol = 10:1, the D-Mannitol typical peak at 166.0°C was suppressed and the formation of a new peak at 133.5°C was observed. When decreasing the ratio (ZnO: D-Mannitol = 4:1), the peaks at 164.1 and 175.5°C indicate the presence of D-Mannitol (table 1, fig. 1). The shift compared to that of raw D-Mannitol (166.0°C) may be explained by the formation of the ZnO - D-Mannitol composites. The peak at 502.5°C corresponds to the crystal growth of ZnO while the peak at 106.4°C may is due to the elimination of OH^- from the crystalline lattice.

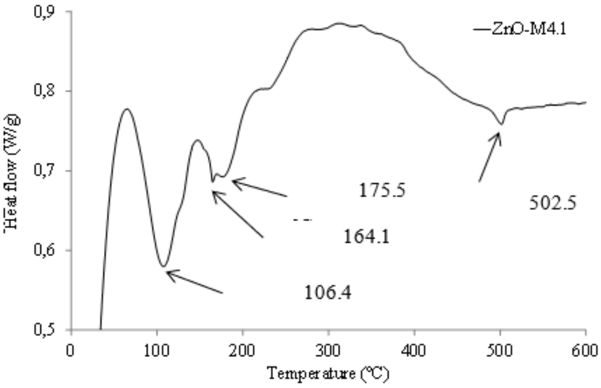

Fig. 1. DSC curve of ZnO-M4.1 synthetized by the solvothermal process

Figure 2 includes the TGA curves obtained for ZnO, D-Mannitol and the microparticles obtained with ratio ZnO: D-Mannitol 10:1 and 4:1 respectively. For the sample ZnO-M10.1, a mass loss of 5.675% corresponding to the elimination of OH^- groups from the lattice can be observed in the temperature range 90.37-162.0°C. In the temperature range 233.72 -500.74°C the mass loss is 35.556% and can be attributed to the decomposition of the transfer charge complex of mannitol and ZnO. The ZnO-M4:1 sample does not show the mass loss of D-Mannitol. This could be explained by the formation of composite structures between the D-Mannitol and ZnO.

The morphology of the microparticles with the different ZnO: D-Mannitol was determined by optical microscopy (fig. 3) and SEM (fig. 4). SEM pictures of ZnO-M10:1 revealed the needle like shape morphology attributed to D-Mannitol and spherical shape morphology of the microcapsule.

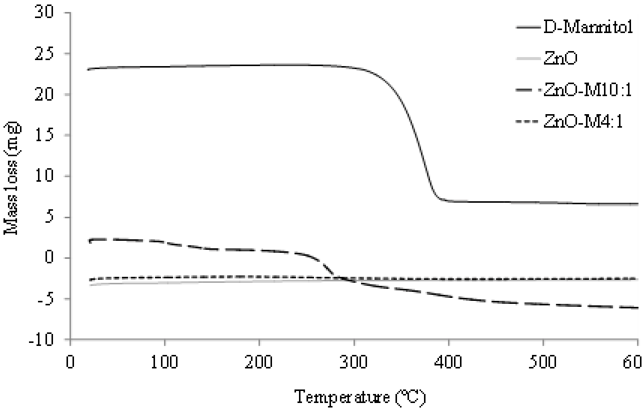

Fig. 2. TGA curves for D-Mannitol, ZnO and microcapsules with ZnO:D-Mannitol ratio 10:1 and 4:1.

Table 1
REPRESENTATIVE SAMPLES PREPARED BY/SOLVOTHERMAL ROUTE FOLLOWED BY SPRAY DRYING PROCESS

SAMPLE	ZnO:D-Mannitol molar ratio	Tm (°C)	ΔHm (J/g)
D-Mannitol		166.0	260.1
ZnO-M10.1	10:1	133.5	2.166
ZnO-M4.1	4:1	164.1 / 175.5	37.91 / 38.46

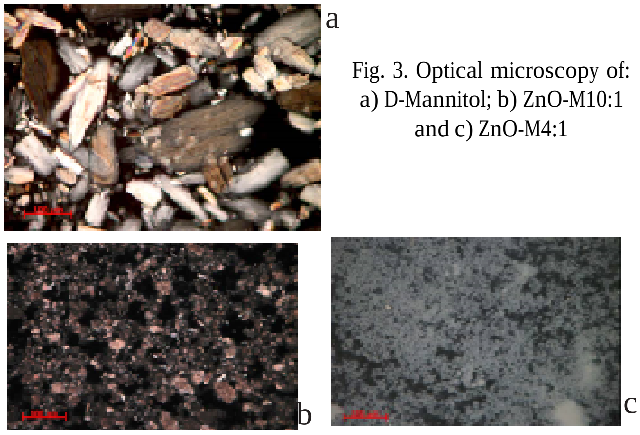

Fig. 3. Optical microscopy of: a) D-Mannitol; b) ZnO-M10:1 and c) ZnO-M4:1

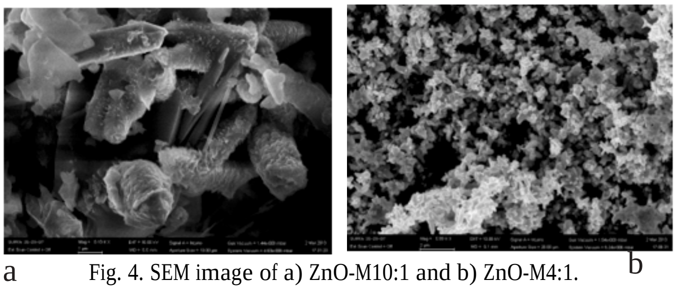

Fig. 4. SEM image of a) ZnO-M10:1 and b) ZnO-M4:1.

In order to deeply analyse the influence of pressure during the solvothermal process on the properties of microparticles, the ratio ZnO: D-Mannitol = 4:1 was selected, using different pressures (1000-3000 atm) and reaction times (1-3 h) at 100°C. Table 2 includes the reference of the samples prepared.

Table 2
REPRESENTATIVE SAMPLES PREPARED FOR MOLAR RATIO ZnO: D-MANNITOL = 4:1

Sample	Synthesis conditions
M1K	1h, 1000 atm, solvothermal
M2K	1h, 3000 atm, solvothermal
M3K	3h, 1000 atm, solvothermal
M4K	3h, 3000 atm, solvothermal

Figure 5 and 6 present the XRD pattern and DSC spectra of the 4 samples obtained.

Characterization of M1K samples prepared at 1000 atm, during 1h at 100 °C.

The SEM images of sample M1K revealed the existence of round shaped nanoparticles of ZnO/mannitol with size range between 48-205 nm (fig. 7). β-D-Mannitol and hexagonal ZnO were identified by XRD (fig. 5a) according to PDF References 01-070-8070 for ZnO and 00-022-1797 for β-D-Mannitol ($C_6H_{14}O_6$). Average crystallite size of ZnO nanoparticles was determined as 29 nm. FT-IR analysis (fig. 8) showed that mainstretching and deformation vibrations of O-H and C-H groups from D-Mannitol, with main characteristics peaks at 1210, 1081, 1018, 959 and 929 cm^{-1} that may be assigned to b-Mannitol [17, 40]. These results agree with DRX characterization.

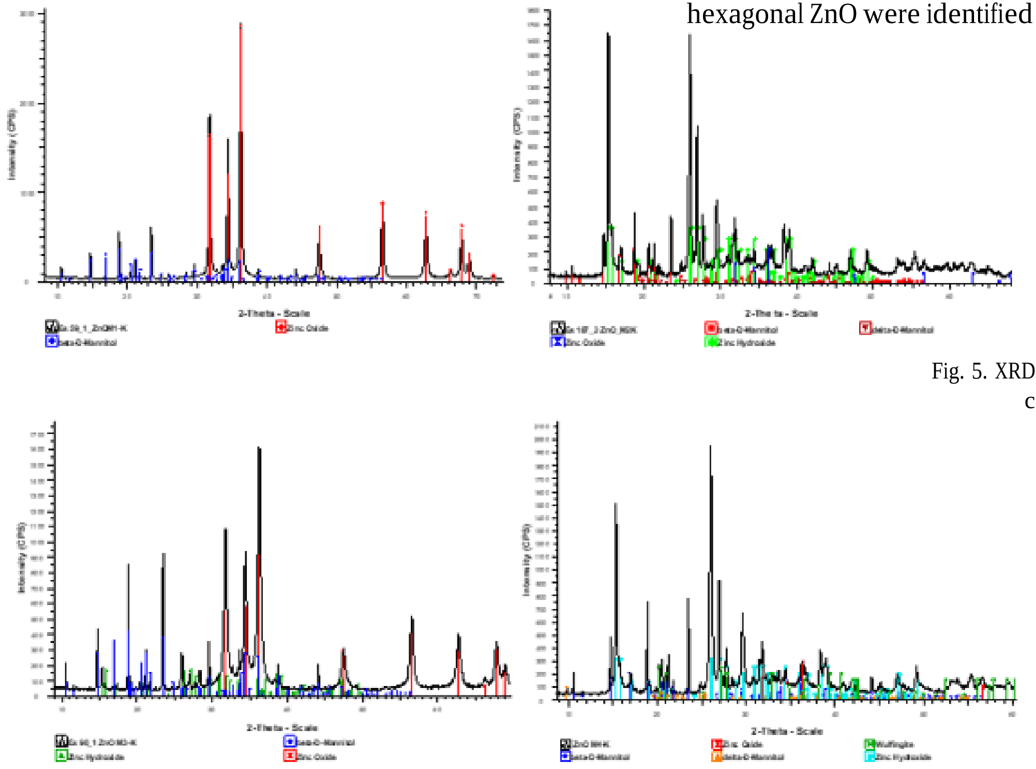

Fig. 5. XRD patterns of a) M1K, b) M2K, c) M3K and d) M4K.

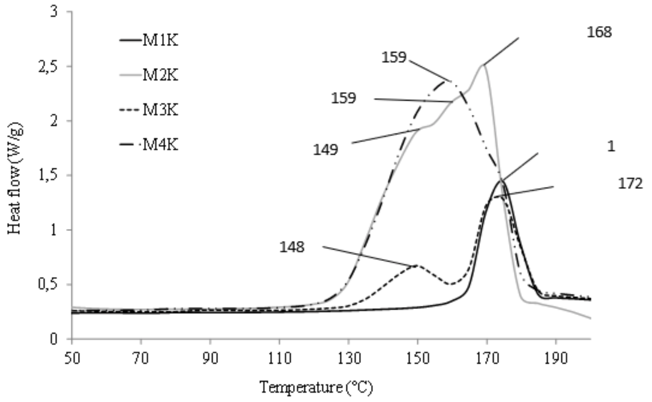

Fig. 6. DSC spectra of M1K, M2K, M3K and M4K

Characterization of M2K samples prepared at 3000 atm, during 1h at 100°C

XRD presented in figure 5b revealed the formation of zinc hydroxide as major phase. Zinc oxide and D-Mannitol were also identified, the latter crystallized as β- and δ-Mannitol. According to XRD results, the higher pressure used for the encapsulation process favours the formation

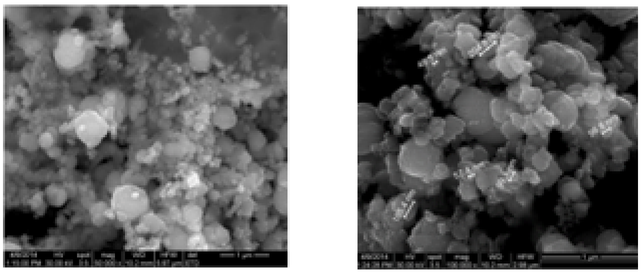

Fig. 7. SEM micrographs of ZnO/D-Mannitol=4:1, 1000 atm, 1h, 100°C.

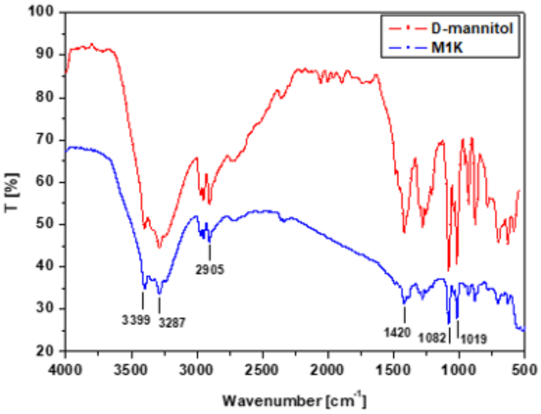

Fig. 8. FT-IR spectra of M1K and D-mannitol

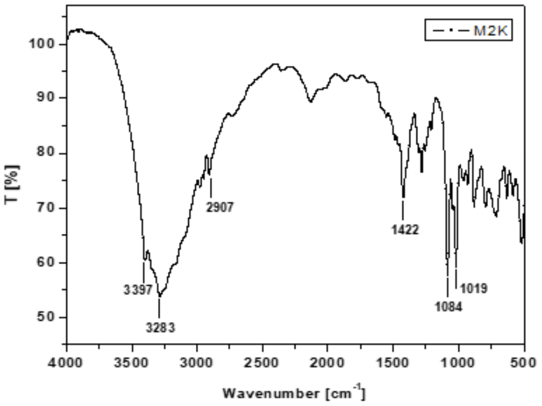

of ZnO and δ-Mannitol, which are not present for lower pressure (M1K). FTIR analysis in figure 9 shows the main molecular vibrations of D-mannitol (stretching and deformation vibrations of O-H and C-H groups).

These results agree with the thermal characterization by DSC (fig. 6), obtaining different melting peaks for the crystalline forms of D-Mannitol (159.6 and 168.5°C and for δ- and β- Mannitol, respectively [17, 41]). The endothermic peak at 149.6

C in the DSC spectra for M2K can be assigned to the OH lattice elimination. Thus, comparison between M1K and M2K indicates that the higher pressure during the encapsulation process favours the presence of zinc hydroxide and δ- Mannitol.

Characterization of M3K samples prepared at 1000 atm, during 3h at 100°C

Figure 5c shows the XRD spectrum of ZnO-mannitol sample. Both ZnO and β-D-Mannitol were identified. Zinc hydroxide is present as a secondary phase.

The longer time for the encapsulation process does not seem to affect crystalline phase transformation, obtaining - Mannitol in both M1K and M3K (1000 atm and 1 and 3 h time, respectively). However, although as a minor component, zinc hydroxide has been formed, as observed in XRD analysis and thermal characterization by DSC (peak at 148.8°C could be ascribed to OH lattice elimination, fig. 6). Second peak (172.4 °C) corresponds to the melting of β- Mannitol.

Characterization of M4K samples prepared at 3000 atm, during 3h at 100 °C

XRD presented in Figure 5d revealed the formation of zinc hydroxide as major phase. Wulfingite, β- and δ-Mannitol and possible peaks of ZnO were also identified. Both the higher pressure and longer times effects previously described can be observed: formation of zinc hydroxide as major phase for higher pressure and the presence of δ-Mannitol. It is also observed that the b β/δ ratio changes when increasing the reaction time (M4K versus M2K). According to DSC characterization (fig. 6, table 3), for the shorter time (1h, sample M2K), the presence of β- Mannitol predominates over δ- phase. However, contrary results can be observed for M4K (3h reaction time) obtaining only a shoulder at 174.7°C and major δ-phase Mannitol (159.6°C).

Table 3 includes quantitative results for melting temperature and enthalpy of the different samples prepared. The endothermic peak at 168-170°C due to the melting of D-Mannitol can be found in the sample M1K at 174 °C.

Table 3

THERMAL PROPERTIES (MELTING TEMPERATURE AND ENTHALPIES (Tm, ΔHm)) OBTAINED BY DSC FOR M1K, M2K, M3K AND M4K

Sample	Tm (°C)	ΔHm (J/g)
M1K	174	56
M2K	149.6; 159.6; 168.5	272
M3K	148.8; 172.4	12.72; 46.56
M4K	159.6; 174.7 (minor)	270.7

Considering melting enthalpies of the different samples, it is clearly observed that M2K and M4K are those with higher thermal energy storage capacity. However, melting enthalpy values are very similar for these samples, therefore 1 h reaction time seems to be enough for the encapsulation, as no thermal enhancement is produced for longer reaction times (M4K).

Conclusions

Microencapsulation of D-Mannitol has been carried out by a solvothermal process at different ZnO: D-Mannitol ratios and pressures. In the low pressure range 40-100 atm. and the highest ratio ZnO: D-Mannitol = 10:1, the D-Mannitol typical peak from 166.0°C disappeared and the formation of a new peak at 133.5°C was observed. Inhomogeneous samples with poor encapsulation degree were formed. When decreasing ZnO:D-Mannitol ratio to 4:1 the peaks at 164.1 and 175.5 °C indicate the presence of D-Mannitol.

Based on XRD analysis, the higher pressures (3000 atm.) favours the formation of zinc hydroxide and δ- Mannitol, instead of the β- Mannitol obtained at lower pressure (1000 atm). These results could be correlated with DSC curves, where an endothermic peak corresponding to OH^- groups elimination from the lattice was observed near 148°C in all these cases (M2K, M3K, and M4K), as well as the peak at 158°C ascribed to δ- Mannitol for M2K and M4K. The longer time during encapsulation process does not seem to affect the crystalline phase transformation of D-Mannitol (the most stable β- Mannitol phase is obtained for both 1 and 3 h reaction time).

Acknowledgements: We gratefully acknowledge the financial support received from European Commission and Romanian Government-Management Authority from Ministry of Research and Innovation, in the frame of Competiveness Operational Program, Action A1.1.4-E-2015, project ID P_37_776, SMIS code 104730, Acronym ENERHIGH and from European Commission in the frame of FP7-296006 SAM.SSA.

References

1.YIN, D., MA, L., LIU, J., ZHANG, Q., Energy, **64,** 2014, 575-581.
2.GIL, A., BARRENECHE, C., MORENO, P., SOLE, C., FERNANDEZ, A. I., CABEZA, L.F., Applied Energy, **111**, issue C, 2013,1107-1113.
3.KUMARESAN, G., VELRAJ, R., INIYA, S., .Journal of Applied Sciences, **11**, 2011, 3044-3048.
4.SHUKLA, A., BUDDHI, D., SAWHNEY R. L., Renewable Energy, **33,** 2008, 2606-2614.
5.KENISARIN, M., MAHKAMOV, K., Renewable Sustainable Energy Rev. **11**, 2007, 1913–1965.
6.PREMKUMAR, M., RAMACHANDRAN, S., European Journal Scientific Research, **1**, 2012, 31-40.
7.SARI, A., Energy Conversion and Management, **64**, 2012, 68-78.
8.FANGA, G., LI, H., YANGA, F., XU LIU, S. WU, Chemical Engineering Journal, **153**, 2009, 217-221.
9.FUENSANTA, M., PAIPHANSIRI, U., ROMERO-SANCHEZ, M.D., LÓPEZ, C. G., LOPEZ BUENDÍA, A.M., LANDFESTER, K., Thermochimica Acta, **565**, 2013, 95-101.
10. KAIZAWA, A., MARUOKA, N., KAWAI, A., KAMANO, H., JOZUKA, T., SENDA, T., AKIYAMA, T., Heat Mass Transfer, **44**, 2008 763-769.
11.BARRENECHE, C., GIL, A., SHETH, F., FERNANDEZ, A. I., CABEZA, L.F., Solar Energy, **94**, 2013, 344-351.
12.HAWLADER, M.N.A., UDDIN, M.S., KHIN, M.M., Applied Energy, **74**, 2003, 195–202.
13.QIU, X., LI, W., SONG, G., CHU, X., TANG, G., Solar Energy Materials and Solar Cells, **98**, 2012, 283-293.
14.JAMEKHORSHID, A., SADRAMELI, S.M., FARID, M., Renewable and Sustainable Energy Reviews, **31**, 2014, 531-542.
15.VENKATA N., JYOTHI, N., PRASANNA, P. M., SAKARKAR, S. N., PRABHA, K.S.,RAMAIAH, P.S., SRAWAN, G.Y, Journal of Microencapsulation, **27 (3)**, 2010, 187–197.
16.ZHAO, C.Y., ZHANG, G.H., Renewable and Sustainable Energy Reviews, **15**, 2011, 3813-3832.
17.QIU, X., LI, W., SONG, G., X. CHU, X., G. TANG, G., Energy, **46 (1)**, 2012, 188-199.
18.CRESPY, D., STARK, M., HOFFMANN-RICHTER, C., ZIENER, U., LANDFESTER, K., Macromolecules, **40**, 2007, 3122-3135.
19.SALAÜN, F., BEDEK, G., DEVAUX, E., DUPONT, D., Materials Letters, 2011, **65**, 381-384.
20.TORINI, L., ARGILLIER, J. F., ZYDOWICZ, N., Macromolecules, **38**, 2005, 3225-3236.
21.ZHAO, C.Y., ZHANG, G.H., Renewable and Sustainable Energy Reviews, **15 (8)**, 2011, 3813-3832.
22.SOUGUIR, H., SALAUN, F., DOUILLET, P., VROMAN, I., CHATTERJEE, S., Chemical Engineering Journal, **221**, 2013, 133-145.
23.SONDARI, D., SEPTEVANI, A. A., RANDY, A., TRIWULANDARI, E., International Journal of Engineering and Technology, **2 (6),** 2010, 466-471.
24.BADWAIK, V.D., VANGALA, L.M., PENDER, D.S., WILLIS, C.B., AGUILAR, Z.P., GONZALEZ, M.S., DAKSHINAMURTHY, R., Nanoscale Research Letters, **7**, 2010,623.
25.PRABHU, B.M., ALI, S.F., MURDOCK, R.C., HUSSAIN, S.M., SRIVATSAN, M., Nanotoxicology, **4**, 2010 150–160.
26.MORONES, J.R., ELECHIGUERRA, J.L., CAMACHO, A., HOLT, K., KOURI, J.B., RAMIREZ, J.T., YACAMAN, M., J. Nanotechnology, **16**, 2005, 2346-2353.
27.XIONG, M.N., GU, G.X., B. YOU, B., Journal of Applied Polymer Science, **90**, 2003, 1923.
28.TANG, E., CHENG, G., MA, X., **161**, 2006, 209-214.
29.ZHOU, H., FAN, T., ZHANG, D., Microporous and Mesoporous Materials, **100**, 2007 322-327.
30.SELVI, N., SANKAR, S., Int.J. Chem.Tech. Res., **6(14)**, 2014, 5665-5671.
31. AGUIRRE, M.E., RODRIGUEZ, H.B., ROMAN, E. S., FELDHOFF, A., GRELA, M.A., J. Phys. Chem. C, **115 (50)**, 2011, 24967-24974.
32.SARKAR, A., SINGH, A.K., KHAN, G.G., SARKAR, D., MANDAL, K., **RSC Adv., 4**, 2014, 55629-55634.
33.PETCHTHANASOMBAT, C., TIENSING, T., SUNINTABOON, P., Journal of Colloid and Interface Science, **369**, 2012, 52-57.
34. KAUSHIK, A., KHAN, R., SOLANKI, P.R., PANDEY, P., ALAM, A., AHMAD, S., MALHOTRA, B.D., Biosens. Bioelectron. **24**, 2008, 676.
35.KELLY, L.K., CORONADO, E., ZHAO, L., SCHATZ, G.C., J Phys Chem B, **107**, 2003, 668-677.
36.AUFFAN, M., BOTTERO, Y.J., CHANEAC, C., ROSE, J., Nanomedicine, **5**, 2010, 999-1007.
37.J. LIAN, Y. LIANG, F. KWONG, Z. DING, H.L. DICKON, Materials Letters, **66**, 2012, 318-320.
38.LITTRINGER, E.M., PAUS, R., MESCHER, A., SCHROETTNER, H., WALZEL, P., URBANETZ, N.A., Powder Technology, **239**, 2013, 162–174.
39.BRUNI, G., BERBENNI, V., MILANESE, C., GIRELLA, A., COFRANCESCO, P., BELLAZZI G., MARINI, A., Journal of Thermal Analysis and Calorimetry, **95 (3**), 2009, 871–876.
40.BURGER, A., HENCK, J.O., HETZ, S., ROLLINGER, J.M., WEISSNICHT, A.A., STOTTNER, H., J. Pharm. Sci. **89**, 2000, 457-468.
41. PITKANEN, I., PERKKALAINEN, P., RAUTIAINEN, H., Thermochim, Acta 214, 1993, 157-162.

Manuscript received: 6.01.2018